The Influence of Imperfections on the Strength and Stability of Cold-Formed Sigma Channels with Corrugated Flanges

Jakub Kasprzak and Piotr Paczos(✉)

Faculty of Mechanical Engineering and Management,
Poznań University of Technology, Poznań, Poland
piotr.paczos@put.poznan.pl

Abstract. Cold-formed, thin walled beams are popular structural members. They are made of thin, cold-rolled steel sheets by using cold-rolling or edge bending machines. The dimensional accuracy of those beams is dependent on manufacturing machines, which can be manually or numerically controlled, and the experience of their operators. If the cross-section of beam is complicated, the actual beams may differ from their idealized counterparts. In this paper the influence of actual imperfections on the strength of sigma channels with corrugated flanges was evaluated. The actual beam was scanned using a high resolution camera and then the generated cloud of 3d points was converted into a surface model using OPTOCAD software. The strength and stability of actual and ideal beams subjected to pure bending were analysed using Finite Element Method. The presented numerical model included material and geometrical nonlinearity that is typical for thin-walled structural members. The obtained results, i.e. critical moment, stresses and deflections, were compared with each other. The influence of the beam length on the results was also evaluated.

Keywords: Cold-formed thin-walled sigma channels · Imperfections · Distortional buckling · Finite element analysis

1 Introduction

Thin-walled, cold-formed structural members, such as beams, are popular constructional elements due to their many advantages. They are made of single steel sheet that may be protected against corrosion. Cold-forming process does not damage this coating so final products, i.e. beams/profiles, do not requires galvanization, powder coating or other anti-corrosion techniques. Cold-formed channels are usually produced on CNC cold-rolling machines, though short series of custom beams can be easily manufactured by using edge bending machines. This makes it possible to produce beams having big cross-sections but small wall-thickness or beams with sophisticated cross-sections. Unfortunately, their load capacity is usually restricted by different forms of buckling. Therefore, some stiffeners are introduced in their flanges or webs. However, the more complicated is the shape of the cross-section, the bigger is the risk of imperfections. This may result in reduced load capacity of beams.

B. Gapiński et al. (Eds.): *Advances in Manufacturing II* - Volume 4, LNME, pp. 36–49, 2019.
https://doi.org/10.1007/978-3-030-16943-5_4

The influence of imperfections on the strength and stability of thin-walled structures is the subject of many scientific works. Ungureanu and Dubina [1], for example, analysed the influence of imperfections on the behaviour of perforated pallet rack members in compression using non-linear finite element simulations. The effect of imperfections, perforations and buckling modes reduced significantly the capacity of perforated members in compression, especially in the coupling range because of interactions between different bucking modes. Rasmussen and Hancock [2] proposed numerical models to generate automatically geometrical imperfection modes into the non–linear analysis.

Experimental and numerical investigations on thin-walled beams, in which actual beams were compared with their idealized models, were conducted by some researchers. Such approach was taken by e.g. Magnucka-Blandzi and Magnucki [3], who improved their mathematical models of beams by comparing theoretical results with experimental ones. They also prepared a review of papers on steel cold-formed structures. Similar problems were analysed by other researches and some results in this field were presented by Magnucka-Blandzi et al. [4] and Paczos et al. [5–7]. They showed their own experimental and numerical investigations of thin-walled channel beams with non-standard cross-sections. Cold formed steel beams with C-, I-, R- and 2R-shaped cross-sections were investigated experimentally (four-point bending test) and numerically by Laim et al. [8].

The extensive review of recent papers on cold-formed structures that were published in leading scientific journals and presented at the main international conferences in the area was presented by Hancock [9].

In this paper, the influence of actual imperfections on the strength and stability of sigma channel beams with corrugated flanges was analysed using non-linear finite element analysis. The numerical model of actual beam was obtained by using 3d optical, measuring system and OPTOCAD software. The results of numerical simulation of actual, scanned beam and its idealized counterpart subjected to pure bending were compared with each other.

The use of high resolution optical systems to analyse thin-walled structures has been growing in recent years including stresses and strain measurements. Such system was used by Paszkiewicz and Kubiak [10] who considered stability of composite channel section beams subjected to pure bending and uniform compression. They used strain gauges, Aramis 3D optical system and a universal testing machine to measure strains and determine critical loads.

2 Beams

This research was devoted to cold-formed thin-walled sigma channel beams with corrugated flanges. The cross-section of beams was presented in Fig. 1.

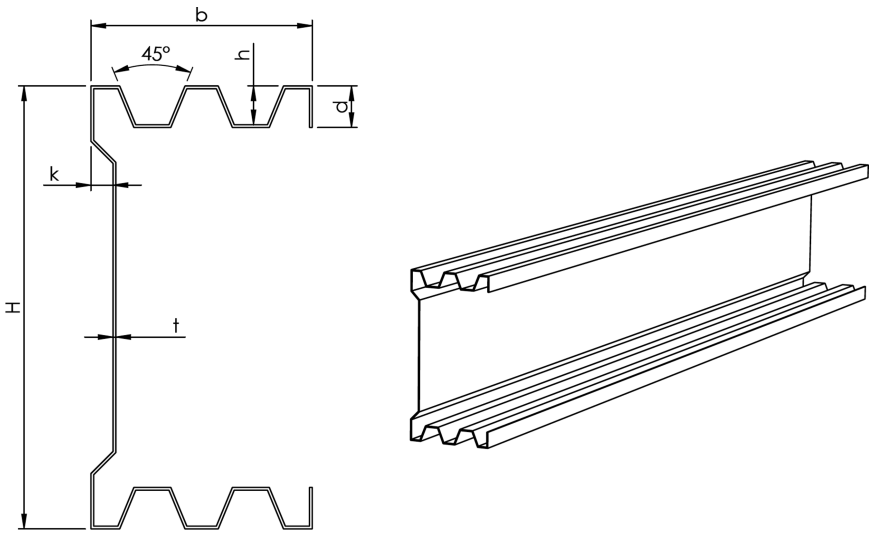

Fig. 1. The cross-section of beam.

The dimensions of beams and their-cross sections were following:

- L = 500, 750 & 1000 mm the total length of beam,
- H = 160 mm the height of beam,
- b = 80 mm the depth of beam,
- h = 14 mm the height of flange corrugation,
- d = 15 mm the height of lip,
- t = 1 mm the wall-thickness of beam,
- k = 8 mm the height of web stiffener.

Those beams may be manufactured by using cold-rolling machines or edge bending machines. The latter are used mainly in the case of short series. Although, they are popular and well-known manufacturing techniques, they also have some disadvantages. One of them is the accuracy of results, i.e. the actual cross-section of beam may be different than the ideal one shown in Fig. 1. In order to evaluate their possible influence on the strength and stability, the actual beam manufactured on an edge bending machine was scanned using SmartScan-HE R8 system.

The scanning process consisted of three stages. In the first, preliminary stage a beam was sprayed with matt paint to prevent light reflection. Afterwards, a few reference points were marked on the scanned beam to compare photos taken from different angles. In the second stage, the beam was scanned using a high-resolution camera. Patterns of strips were displayed on the surface of beam and then pictures were

taken. In the third stage, obtained data was processed by a computer. At the beginning, the cloud of X, Y, Z points was generated in OPTOCAD software. Then they were converted in CATIA v5 to a surface model that could be directly exported to CAD and FEA software. The scanning was done by external company specialized in such a kind of optical measurements.

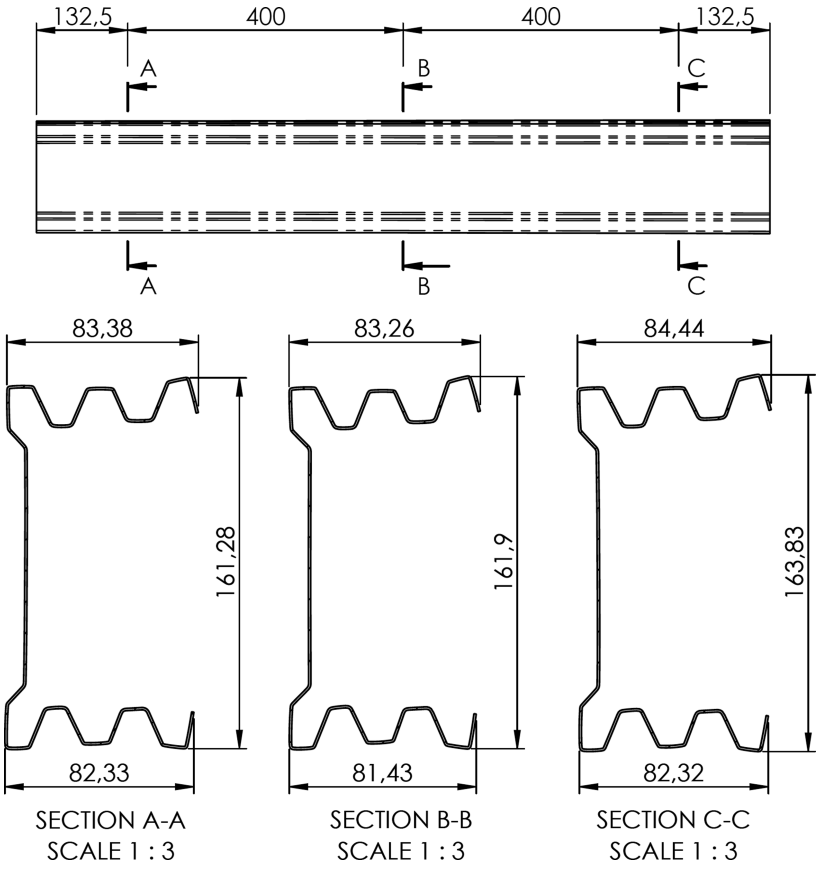

Fig. 2. The actual cross-sections of scanned beam.

Cross-sections of the scanned beam were presented in Fig. 2. The actual cross-sections differed from the ideal one. In order to compare the geometrical properties of actual and ideal cross-sections, the 3d model of scanned, actual beam was cut in eleven points (spaced evenly along the beam). Then the geometrical properties of each cross-section were measured using CAD software. The obtained results were compared with

the geometrical properties of ideal cross-section. The relative difference between the actual and ideal principal moments of inertia along the beam was shown in Fig. 3. The first, actual, principal moment of inertia was smaller by 1–4.2% than its ideal counterpart. The second, actual, principal moment of inertia at the ends of beam was bigger than ideal one (max. by 2.3%), but in the centre of beam it might be 1.3% smaller. The differences between the elastic section moduli was similar. The angle between the principal and global beam axes varied form 0.36° at one end to 0.98° at another one.

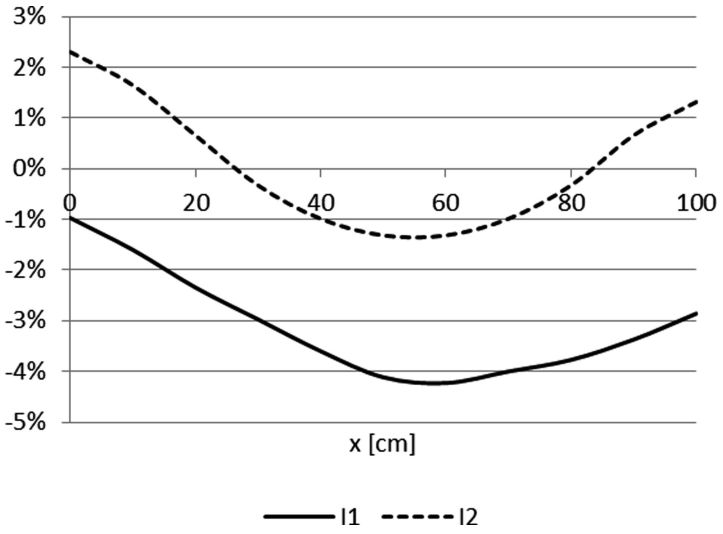

Fig. 3. The difference between the actual and ideal principal moments of inertia along the beam.

3 Numerical Model

The strength and stability of actual, scanned and ideal beams were evaluated using SolidWorks Simulation Premium 2012 FEA software integrated with popular SolidWorks 2012 CAD system. Channel beams are usually subjected to bending loads so in this case simply supported beams subjected to pure bending were analysed to avoid their twisting and local effects of point loads. Thin-walled beams were modelled using the second order triangular elements that consisted of six nodes (3 vertices and 3 midnodes) and three parabolic edges. In this way the curvature of edge radiuses could be accurately modelled. The finite element mesh of the actual, scanned 1 m beam was

presented in Fig. 4. The maximum size of elements was 10 mm. There were 26 895 nodes and 13 250 elements. In preliminary analyses smaller 5 mm elements were used as well, but the obtained results differed from the presented ones by less than 1%. The mesh of ideal 1 m beam consisted of 18 009 nodes and 8 840 elements. Their smaller number was the result of neglecting edge radiuses in the model.

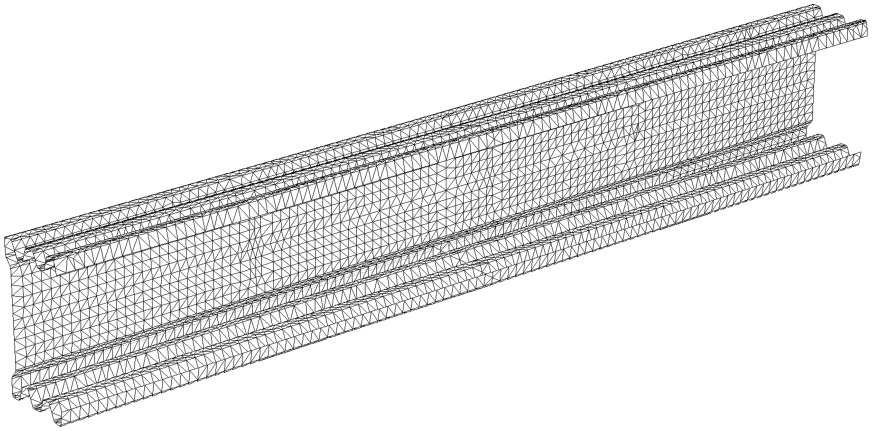

Fig. 4. Scanned, actual beam L = 1000 m: finite element mesh (max. size of elements 10 mm).

The cross-section of thin-walled channels may change its shape during bending. Therefore, numerical model included geometrical and material nonlinearity. In other words, the stiffness matrix was updated at each iteration step and plastic von Mises model of material was based on the true stress-strain curve (Fig. 5) determined from tensile tests of specimens cut from the web of beam. It is noteworthy that strains in the considered cases were less than 0.2%. Therefore, only the small part of the curve was used.

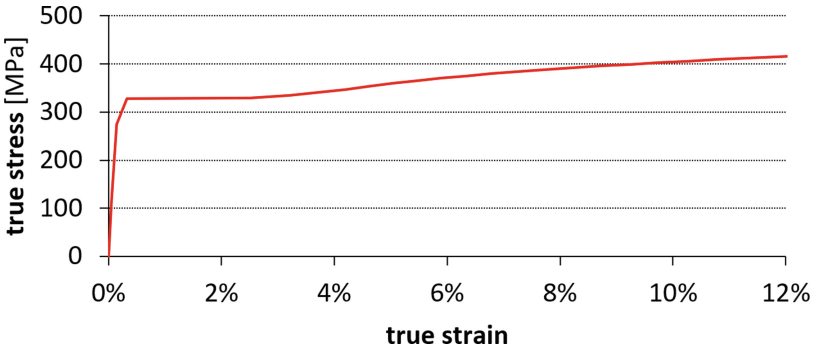

Fig. 5. True stress-strain curve used in the presented numerical calculations (the limit of proportionality σ_p = 115 MPa, the yield strength σ_a = 328 MPa).

Bending moments were simulated as pressure applied to the end cross-section of beams. They acted in the direction parallel to the beam axis. The value of pressure changed linearly from 0 at the neutral axis of beam to max/min values at the ends of beam (Fig. 6). The following boundary conditions were applied to numerical models of beams to avoid local effects at the supports. At both ends of beams, displacements in plane perpendicular to the beam axis were locked ($u_y = u_z = 0$). Moreover, displacements parallel to the beam axis were locked along the centre of the web (Fig. 6). Critical load and ultimate strength are usually very dependent on assumed boundary conditions so only beams having exactly the same boundary conditions could be compared.

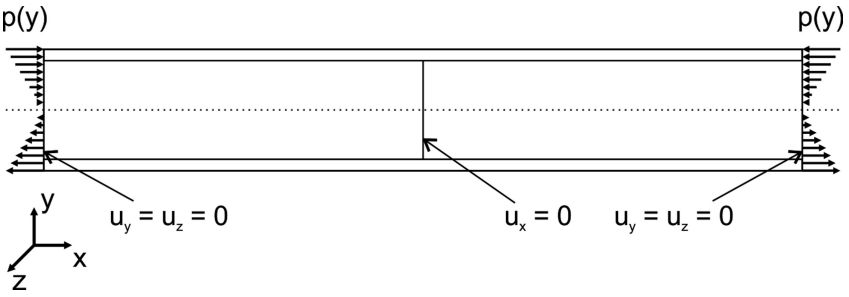

Fig. 6. Load and boundary conditions of beams.

4 Results of Numerical Simulations

The actual, scanned and ideal beams were analysed until they collapsed. Three different lengths of beams were considered: 0.5, 0.75 and 1.0 m. This was done to evaluate if the length of beam influenced results, i.e. if imperfections had smaller effect in short/long beams.

The considered ideal channel beams collapsed because of elastic distortional buckling. In other words, the deflection of the top compressed flange increased much quicker than the rest of beam and when stresses reached the critical value, beam collapsed. This could seen in Fig. 7 where deflection in the middle of ideal 1 m beam versus bending moment in four points was shown. The deflection of each corner was a bit different even for small values of bending moment. The deflection of the top, compressed flange (point B) was the biggest one. The vertical displacements in the top and bottom corners of the web at the beginning were the same, but for M = 0.656 kNm started to differ. The deflection of the bottom flange increased slowly and for M = 2.0 kNm started to decrease.

The buckling (distortional) mode of ideal 1 m beam was shown in Fig. 8. The deformation of the top compressed flange was also visible in stress plots shown in Fig. 9. The stresses in the top flange were not uniform, as one may expect using classical beam theory. Higher stresses were observed at the centre of top, compressed flange close to the reinforcing lip. The bottom plot in Fig. 9 showed the stresses just before the collapse of beam. Maximum stresses in this case were equal to 290 MPa and they were lower than the yield strength of the material, i.e. 328 MPa. It meant that the observed buckling mode was actually an elastic one. The top plot presented in Fig. 9 showed 1.0 m actual, scanned beam when stresses were equal to the limit of proportionality.

It is noteworthy that the failure mode was not dependent on the length of beam, i.e. 0.5, 0.75 and 1 m long beam collapsed in the same way – elastic distortional buckling. Naturally, the value of the maximum, critical moment decreased with the length of beam.

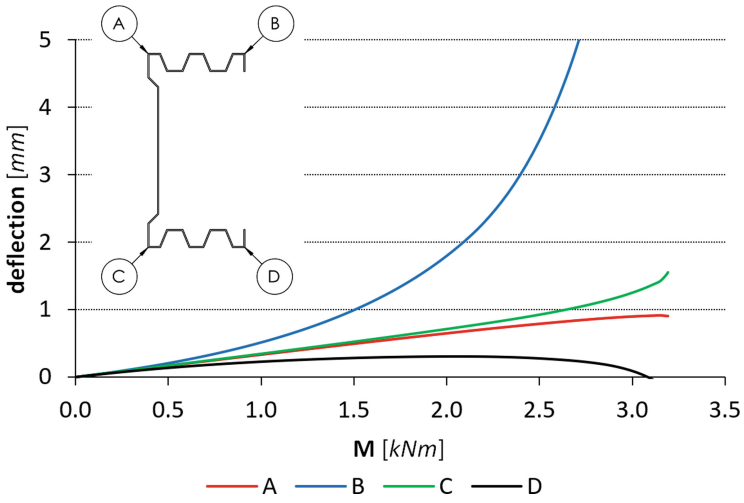

Fig. 7. The relationship between bending moment and deflection of 1 m ideal beam.

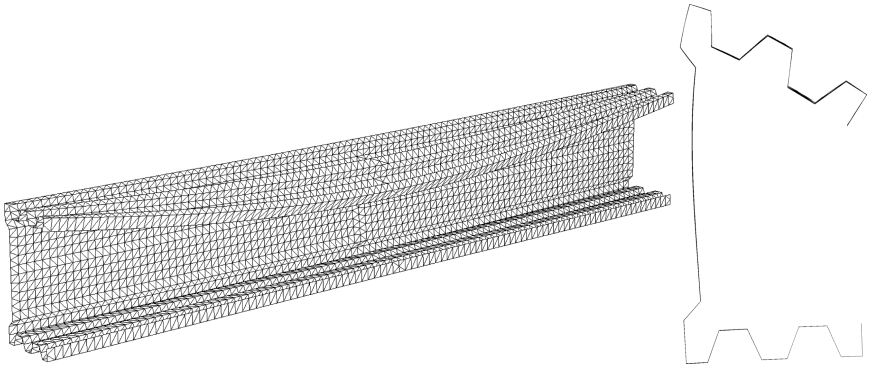

Fig. 8. Distortional buckling mode of the ideal 1 m beam (deformation not in scale).

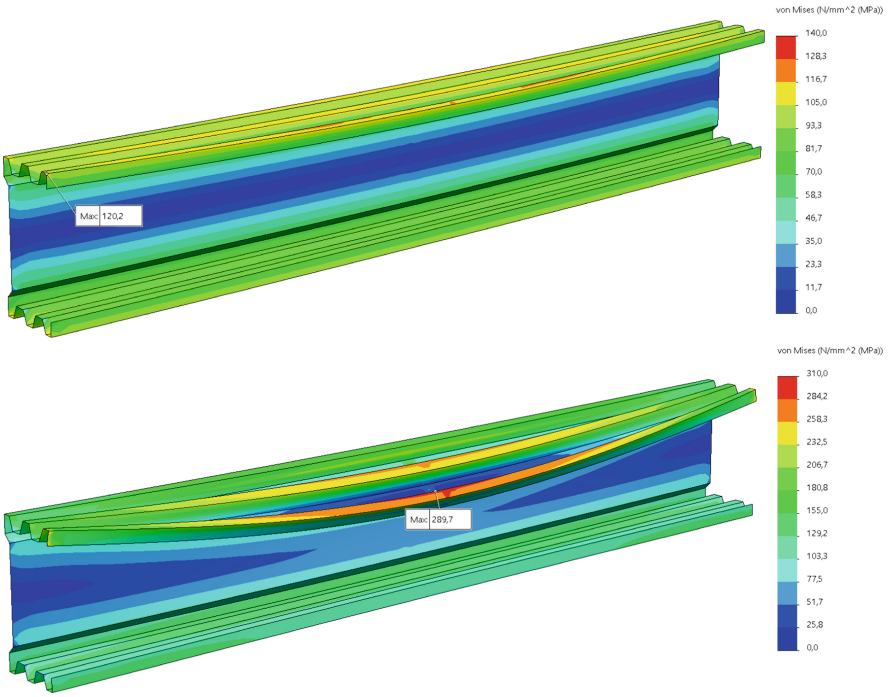

Fig. 9. Von Mises stresses at the outer surface of ideal 1 m beam: top plot M = 2.13 kNm, bottom plot M = M_{max} = 3.19 kNm (deformation not in scale).

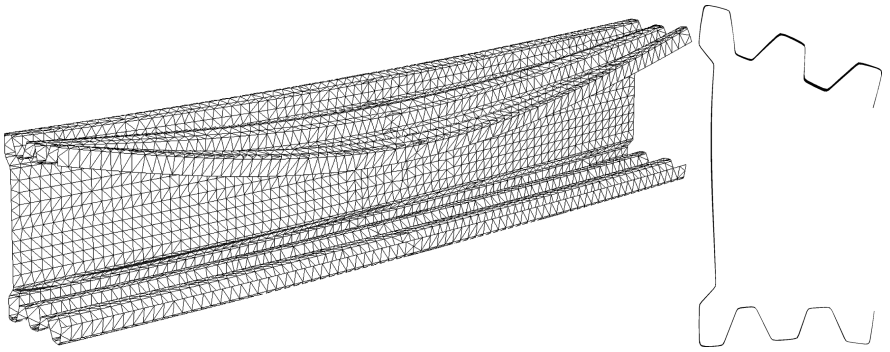

Fig. 10. Distortional buckling mode of the scanned 0.75 m beam (deformation not in scale).

The failure mechanism of actual, scanned beams was the same as ideal ones, i.e. elastic distortional buckling (Fig. 10). However, their maximum, critical bending moment was smaller. The comparison of maximum bending moments of actual, scanned and ideal beams was shown in Table 1. In the considered case, imperfections reduced the maximum bending moment by a few percent (3.0–5.4%). Naturally, the longer was a beam the lower was the maximum bending moment. This was caused by the fact that for the same bending moment the deflection of actual, scanned beam was bigger. The relationship between bending moment and deflection of 0.75 m beams was presented in Fig. 11 – two graphs referring to the top (compressed) and bottom (in

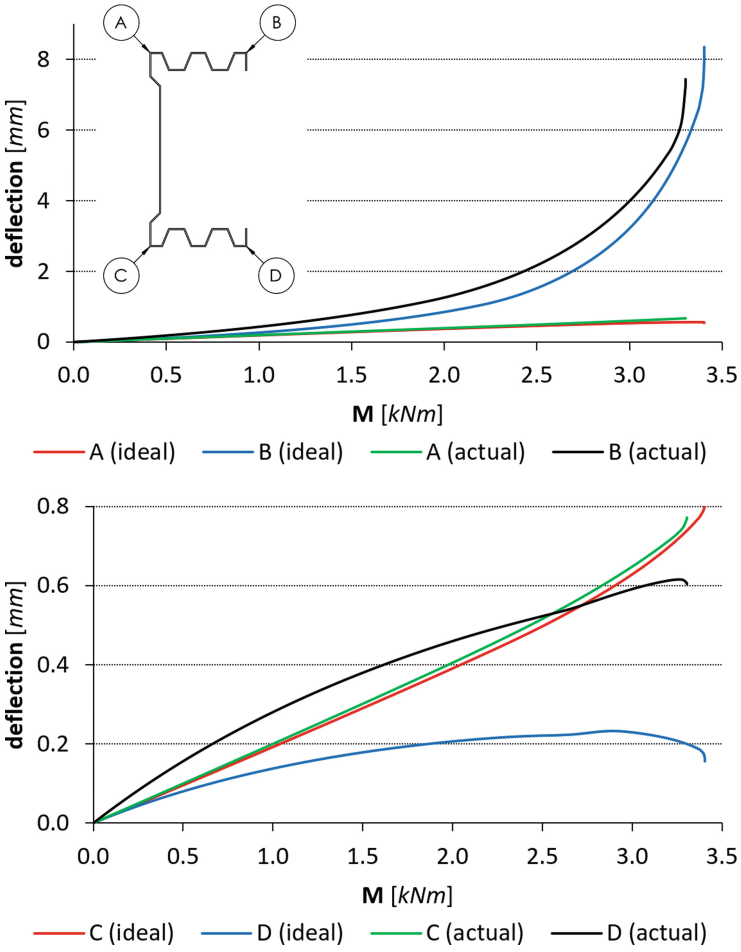

Fig. 11. The relationship between bending moment and deflection of ideal and actual, scanned 0.75 m beams.

tension) flange respectively. The relationships for ideal and actual scanned beams were similar with one exception. The maximum deflection of the bottom flange measured in the middle of actual, scanned 0.75 m beam raised monotonically until collapse. In the case of ideal beam for bending moment bigger than 2.89 kNm the deflection of the bottom flange started to decrease.

Table 1. The comparison of the maximum (limit) M_{max} bending moments.

Length	Ideal beam	Actual beam	Rel. difference
0.50 m	4.654 kNm	4.465 kNm	4.06%
0.75 m	3.404 kNm	3.303 kNm	2.97%
1.00 m	3.190 kNm	3.018 kNm	5.39%

Not only the relationships between bending moment and deflection of ideal and actual, scanned beams were similar. The same referred to von Mises stresses. The relationship between them and bending moment was presented in Fig. 12. The graphs for ideal and imperfect beams were very similar. Naturally, von Mises stresses in the actual, scanned 0.75 m beam for the same bending moment were higher than stresses in ideal beam. In all cases (points) some anomalies were observed, in other words stresses did not increase monotonically with bending moment, but there were steps in graphs. The value of stresses at which those anomalies were observed matched the limit of proportionality, i.e. 115 MPa. There were no such steps in the graphs showing the relationship between deflection and bending moment. Therefore, their nature was rather numerical and they had no physical meaning. They could not be treated as local or any other form of buckling. The maximum stresses in actual, scanned beams exceed the limit of proportionality for smaller bending moments than stresses in the ideal beams. Moreover, the longer was a beam the bigger was the difference. The comparison between "critical bending moments" for which maximum stresses exceed the limit of proportionality was presented in Table 2. The difference between them varied from 8.3% for short 0.5 m beams to 13.8% for long 1.0 m beams.

Table 2. The comparison of the "critical" M_{cr} bending moments.

Length	Ideal beam	Actual beam	Rel. difference
0.50 m	2.362 kNm	2.165 kNm	8.34%
0.75 m	2.187 kNm	1.968 kNm	10.01%
1.00 m	2.132 kNm	1.837 kNm	13.84%

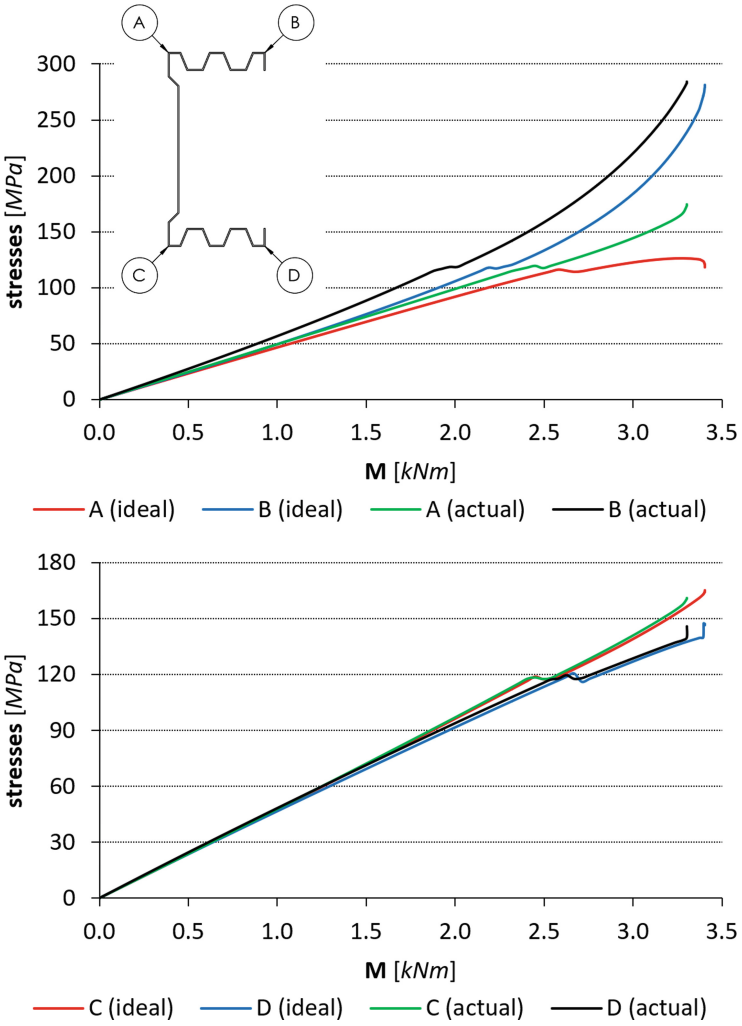

Fig. 12. The relationship between bending moment and von Mises stresses at the outer surface of ideal and actual, scanned 0.75 m beams.

5 Conclusions

In the paper, the influence of imperfections on the strength and stability of sigma channels with corrugated flanges was analysed. The actual imperfections were considered. They were implemented into numerical model by 3d scanning of actual beam. Those imperfections reduced the geometrical properties of cross-section even by 4.2% (the first principle moment of inertia) and rotated the principle axes by 0.98° in relation to the global coordinate system, i.e. an actual profile was not perfectly symmetrical.

Simply supported beams subjected to pure bending were considered, because channels usually carry transverse loads. Preliminary investigations confirmed a well-known fact that such thin-walled, cold-formed channel beams could not be analysed using static linear analysis based on classical beam theory. The stress distribution in the plane parallel to the neutral axis, e.g. in the flange, was not uniform and the shape of cross-section changed as load (bending moment) increased. In order to accurately simulate the behaviour of beams, geometrical and material nonlinearities were included in numerical models. The used true stress-strain curve was based on the actual tensile tests of specimens cut from beams.

The strength and stability of actual, scanned beams were compared with the strength and stability of their idealized counterparts that did not include edge radiuses. In all considered cases, beams collapsed because of elastic, distortional buckling that is typical for short, thin-walled channels with reinforced flanges. Imperfections reduced the maximum bending moment (limit load) by 3.0–5.4% so a little bit more than the geometrical properties of cross-sections. The behaviour of actual, scanned and ideal beams, i.e. relationships between bending moment and deflection or stresses, was very similar with one exception. In the case of ideal 0.75 m beam the deflection of bottom (in tension) flange decreased for $M > 2.89$ kNm, whereas the deflection of the actual bottom flange increased monotonically till collapse.

The anomalies in the relationships between bending moment and von Mises stresses (steps visible in stress-moment graphs, Fig. 12) were rather numerical ones. They were observed for stresses equal to the limit of proportionality, i.e. 115 MPa. The maximum stresses of actual, scanned beam exceeded this limit for smaller values of bending moment than in the case of ideal beams. The difference was equal to 8.3–13.8% and raises for longer beams. It is even three times bigger than the reduction of geometrical properties of cross-section.

In conclusion, in the considered case imperfections did not change the nature of failure (the same bucking mode) but naturally reduced the critical and maximum moments. The relative (percentage) reduction of those loads was much bigger than the reduction of cross-section properties (up to three times).

Acknowledgments. The research work reported here was made possible by support of the National Science Centre given on the decision No. DEC-2017/25/B/ST8/00266 of 2017-11-23 – Contract No. UMO-2017/25/B/ST8/00266.

References

1. Ungureanu, V., Dubina, D.: Sensitivity to imperfections of perforated pallet rack sections. Mech. Mech. Eng. **17**(2), 207–220 (2013)
2. Rasmussen, K.J.R., Hancock, G.J.: Geometric imperfections in plated structures subject to interaction between buckling modes. Thin-Walled Struct. **6**, 433–452 (1988)
3. Magnucka-Blandzi, E., Magnucki, K.: Buckling and optimal design of cold-formed thin-walled beams: review of selected problems. Thin-Walled Struct. **49**, 554–561 (2011)

4. Magnucka-Blandzi, E., Paczos, P., Wasilewicz, P.: Buckling study of thin-walled channel beams with double-box flanges in pure bending. Strain Int. J. Exp. Mech. **48**, 317–325 (2012). Blackwell Publishing Ltd.
5. Magnucki, K., Paczos, P., Kasprzak, J.: Elastic buckling of cold-formed thin-walled channel beams with drop flanges. J. Struct. Eng.-ASCE **136**(7), 886–896 (2010)
6. Paczos, P.: Experimental and numerical (FSM) investigations of thin-walled beams with double-box flanges. J. Theor. Appl. Mech. **51**(2), 497–504 (2013)
7. Paczos, P.: Experimental investigations of thin-walled C-beams with nonstandard flanges. J. Constr. Steel Res. **93**, 77–87 (2014)
8. Laim, L., Rodrigues, J.P.C., da Silva, L.S.: Experimental and numerical analysis on the structural behaviour of cold-formed steel beams. Thin-Walled Struct. **72**, 1–13 (2013)
9. Hancock, G.: Cold-formed steel structures: research review 2013–2014. Adv. Struct. Eng. **19** (3), 393–408 (2016)
10. Paszkiewicz, M., Kubiak, T.: Selected problems concerning determination of the buckling load of channel section beams and columns. Thin-Walled Struct. **93**, 112–121 (2015)